

1
2
3
4
5
6
7
8
9
10
11
12
13
14
15
16
17 **Selectivity sequences in a model calcium channel:**
18 **Role of electrostatic field strength**
19
20
21
22
23
24
25
26
27
28

29 Daniel Krauss^{1,2}, Bob Eisenberg¹, and Dirk Gillespie^{1,*}
30

31
32 ¹Department of Molecular Biophysics and Physiology, Rush University Medical Center,
33 Chicago, IL

34 ²Grinnell College, Grinnell, IA
35
36

37
38 *corresponding author: dirk_gillespie@rush.edu
39
40
41
42
43
44
45
46
47
48
49
50
51
52
53
54
55
56
57

58 24 November 2010
59
60
61
62
63
64
65

ABSTRACT

The energetics that give rise to selectivity sequences of ionic binding selectivity of Li^+ , Na^+ , K^+ , Rb^+ , and Cs^+ in a model of a calcium channel are considered. This work generalizes Eisenman's classical treatment (*Biophys. J.* 2 (Suppl. 2), 259) by including multiple, mobile binding site oxygens that coordinate many permeating ions (all modeled as charged, hard spheres). The selectivity filter of the model calcium channel allows the carboxyl terminal groups of glutamate and aspartate side chains to directly interact with and coordinate the permeating ions. Ion dehydration effects are represented with a Born energy between the dielectric coefficients of the selectivity filter and the bath. High oxygen concentration creates a high field strength site that prefers small ions, as in Eisenman's model. On the other hand, a low filter dielectric constant also creates a high field strength site, but this site prefers large ions, contrary to Eisenman's model. These results indicate that field strength does not have a unique effect on ionic binding selectivity sequences once entropic, electrostatic, and dehydration forces are included in the model. Thus, Eisenman's classical relationship between field strength and selectivity sequences must be supplemented with additional information in selectivity filters like the calcium channel that have amino acid side chains mixing with ions to make a crowded permeation pathway.

INTRODUCTION

If Li^+ , Na^+ , K^+ , Rb^+ , and Cs^+ are placed in equimolar amounts outside a channel and allowed to permeate only 11 of the possible 120 different possible sequences of binding selectivity have been found in actual channels. Eisenman described these selectivity sequences of ion binding in ion channels solely as a function of electrostatics and dehydration (Eisenman 1962; Eisenman and Horn 1983). His first model (Eisenman 1962) ignored many physical properties like entropy that are critical to accurately describe condensed matter systems like an electrolyte in a channel. Despite its simplicity, Eisenman's model has proven to be remarkably accurate at predicting the 11 sequences that occur.

Here we expand on Eisenman's idea. In an early paper he noted that "While it is possible to extend the above calculations [for electrochemical potential] to assess the role of adjacent oxygens, silicons, and "screening" cations, the lack of detailed knowledge of their positions makes it more profitable at present to simplify the above representations by a single charged monopolar site" (Eisenman 1962). In our paper we include these adjacent oxygens and screening charges by modeling the oxygens as half-charged, mobile spheres that can coordinate the permeating ions. We also include a dielectric constant for the binding site to describe ion dehydration. Overall, this allows us to include electrostatics, dehydration, and entropic forces in our characterization of selectivity sequences in calcium channels, the main class of channels to which our model applies. While Eisenman and Alvarez (Eisenman and Alvarez 1991) have studied the effect of nearby channel atoms in some specific channel structures, our approach allows us to *systematically* explore all possible outcomes (within the confines of our reduced model) in a system in which all atoms are at their free energy minimum. This approach then gives a broad brushstroke picture of selectivity sequences in calcium channels.

We observe that the two parameters within our model, the oxygen concentration and the filter dielectric constant, predict a wide range of selectivity sequences. Each parameter can increase the filter field strength, either by increasing oxygen concentration or decreasing the filter dielectric constant. The oxygen concentration creates a typical correlation between the

1
2
3
4 Eisenman sequences and “field strength”. However, the dielectric constant of the filter results in
5 a “high field strength” site that produces a “low field strength” selectivity sequence. Therefore,
6 we conclude that selectivity in a model of a pore crowded with amino acids side chains cannot be
7 characterized by one parameter like field strength. Since ours is a very simple model, we
8 speculate that the same is true in a real channel, a much more complicated system.
9

11 THE EISENMAN MODEL

13 In this section we will give a brief review of the basic Eisenman model (Eisenman 1962),
14 ignoring its many generalizations and extensions (see (Eisenman and Horn 1983) and references
15 therein). Eisenman modeled the alkali ions as equivalent charged spheres with their
16 Goldschmidt radii and the binding site as a sphere with a charge of -1 . This model is based on
17 the physics of ion selective glass electrodes. By simple electrostatic calculations, one can
18 compute the energy of the system to show that the smaller the ion, the higher its affinity for a
19 sphere of that diameter (Eisenman 1962; Hille 2001).
20

21 With just this information, the only selectivity sequence that could be observed would be
22 $\text{Li}^+ > \text{Na}^+ > \text{K}^+ > \text{Rb}^+ > \text{Cs}^+$ (Sequence XI, Table 1). The smaller ion will always be able to move
23 closer to the binding site charge. However, if ions dehydrate before they permeate, Eisenman
24 sequences come from the competition between binding and dehydration, and one can observe a
25 myriad of selectivity sequences. As the size of the binding site sphere changes from small to
26 large, the Eisenman selectivity sequences are observed (Table 1). Eisenman defined a sequence
27 corresponding to a small sphere as a “high field strength” site and those corresponding to a large
28 sphere as “low field strength”. He could then apply “field strength” to actual channels based on
29 their selectivity properties.
30

31 The Eisenman sequences are then the result of two competing phenomena, the attraction
32 of ion into the charged binding site and the dehydration penalty for entering the binding site.
33 Generalizing the work of Krasne and Eisenman (Krasne and Eisenman 1973), Eisenman and
34 Horn (Eisenman and Horn 1983) showed that the sequences arise as long as the attraction term
35 falls off as function of ion size as a lower power than the dehydration term. While this approach
36 is simple in principle, some have criticized this “field strength” argument. Armstrong
37 (Armstrong 1989), for example, demonstrated that the Eisenman procedure is very inaccurate
38 when predicting relative ratios between ions. He also showed that the sequences observed are
39 very sensitive to the particular diameter used. If, for instance, Pauling radii are used in the place
40 of Goldschmidt radii, no K^+ selective channels are observed. This makes it possible that the 11
41 Eisenman sequences do not correspond to Eisenman’s “field strength.”
42

43 As an alternative, Armstrong suggested that any theory that produced a single peak when
44 affinity is plotted as a function of permeant ion radius will produce the Eisenman sequences
45 (plus five others) (Armstrong 1989). The balance of electrostatic attraction and ion dehydration
46 do this since each energy is monotonic in ion radius (but of opposite sign). Later we show that
47 Armstrong’s idea does not hold in our model when the filter dielectric constant is very low.
48
49

53 REDUCED CALCIUM CHANNEL MODEL

54 Our model is an extension of Eisenman’s original work (Eisenman 1962). Selectivity
55 within our model is fundamentally based on a balance of dehydration and electrostatics, just like
56 within his model. Eisenman made clear that he wanted to push his model further to include the
57 roles of multiple pore charges and screening cations, but lacked the structural data, ionic theory,
58 and computational power to do so.
59
60

1
2
3
4 Our reduced model of a calcium channel consists of two bulk fluids (homogeneous and
5 infinite in all directions) consisting of ions modeled as charged hard spheres. Water is implicitly
6 present in each compartment as dielectric constants, one for each fluid. One fluid represents the
7 bath outside the channel and contains the permeating ions. The other fluid represents the
8 selectivity filter and contains a given concentration of half-charged oxygen ions ($O^{1/2-}$). These
9 oxygens represent the carboxyl oxygens present in the selectivity filter of calcium channels or
10 the carbonyl oxygens of the protein backbone of K^+ channels. Koch et al. (2000) have shown
11 that the glutamates of L-type calcium channels face the permeation pathway and therefore can
12 directly interact with the permeating ions.
13

14
15 The oxygens are modeled as a fluid so that they can coordinate the permeating ions,
16 which has been shown to give calcium channels their selectivity (Boda et al. 2000; Boda et al.
17 2002; Gillespie 2008; Nonner et al. 2000). Because the fluid is infinite in all directions, the
18 model makes no distinction between having n oxygens in a filter of volume v and having αn
19 oxygens in a filter of volume αv . Thus, any channel geometry is represented through $[O^{1/2-}]$; the
20 selectivity filter does not have an explicit length or radius.
21

22
23 $[O^{1/2-}]$ also determines selectivity. As an example, $[O^{1/2-}] = 40$ M behaves somewhat like
24 the highly Ca^{2+} selective L-type Ca^{2+} channel while $[O^{1/2-}] = 20$ M behaves more like the mildly
25 Ca^{2+} selective ryanodine receptor calcium channel (Krauss and Gillespie 2010; Nonner et al.
26 2000). Theoretical studies support the assumption that oxygen concentration as opposed to size
27 or shape of the filter determines the number of ions which move into the filter (Malasics et al.
28 2009). By changing the oxygen concentration we alter the charge density of the filter. A higher
29 $[O^{1/2-}]$ therefore results in a higher field strength site.
30

31 The dielectric constant within the filter gives us a way of including water and dehydration
32 (Nonner et al. 2001). If the dielectric constant within the filter is the same as the bath (78.4), all
33 waters of hydration are free to move into the channel, and there are zero penalties for shedding
34 waters of hydration. On the other hand, if the channel's dielectric constant is lower than that of
35 the bath, the channel can better exclude waters of hydration and thus has penalties for shedding
36 waters of hydration. Reducing the filter's dielectric constant also reduces the amount of water
37 between the screening charge and therefore also increases the interactions between the ions and
38 between the ions and the oxygens. This means that a low dielectric constant results in a high
39 field strength site.
40

41
42 While this model is greatly simplified, it has the key selectivity properties of calcium
43 channels (Nonner et al. 2000). This model is by no means quantitatively accurate. However,
44 many studies have shown that, in calcium channels, selectivity is determined primarily by a
45 balance of cations entering the filter to screen the negative amino acids and a lack of space in the
46 crowded filter, exactly the two forces that act on the system within our model (Boda et al. 2000;
47 Boda et al. 2001; Boda et al. 2002; Boda et al. 2008; Boda et al. 2006, 2007; Boda et al. 2009;
48 Gillespie 2008; Gillespie and Boda 2008; Gillespie et al. 2008; Gillespie and Fill 2008; Gillespie
49 et al. 2009; Gillespie et al. 2005; Malasics et al. 2009; Miedema et al. 2004; Miedema et al.
50 2006; Nonner et al. 2000; Nonner and Eisenberg 1998; Nonner et al. 2001; Rodriguez-Contreras
51 et al. 2002). This reduced model of amino acids in the selectivity filter has successfully modeled
52 calcium selectivity in the pores such as the L-type calcium channel and the ryanodine receptor. It
53 has also reproduced and predicted experimental data in many cases (Boda et al. 2009; Gillespie
54 2008; Gillespie and Boda 2008; Gillespie and Fill 2008; Gillespie et al. 2009; Gillespie et al.
55 2005; Miedema et al. 2004; Miedema et al. 2006; Nonner et al. 2000; Rodriguez-Contreras et al.
56 2002).
57
58
59
60
61
62
63
64
65

This system in this paper uses the mean spherical approximation (MSA) to compute the electrochemical potential of these ions (Barthel et al. 1998; Blum 1975; Blum 1980; Nonner et al. 2000; Nonner et al. 2001; Waisman and Lebowitz 1970). Given the bath concentrations, valences, and ionic radii of all the permeating ions and the concentration of oxygens in the filter we can use the MSA theory for the excess chemical potential to determine the concentration of each bath ion in the filter. Since our system is in equilibrium, the chemical potential for all ions is the same for the bath and the filter so that, for ion species X,

$$\begin{aligned} \mu_X^{\text{bath}} = & \overbrace{kT \cdot \ln(\Lambda_X^3 [X]_{\text{filter}})}^{\text{ideal gas}} + \overbrace{z_X V_D}_{\text{mean electrostatic}} + \overbrace{\mu_X^{\text{SC}}}_{\text{screening}} + \overbrace{\mu_X^{\text{HS}}}_{\text{excluded volume}} \\ & + \overbrace{\mu_X^{\text{dehydr}} \frac{\epsilon_{\text{filter}} - \epsilon_{\text{bath}}}{\epsilon_{\text{filter}} (\epsilon_{\text{bath}} - 1)}}^{\text{dehydration}} \end{aligned} \quad (1)$$

where μ_X^{bath} is the electrochemical potential of the ion in the bath, k_B is the Boltzmann constant, T is temperature in Kelvin, $[X]_{\text{filter}}$ is concentration of the ion in the filter, z_X is valence, V_D is Donnan (electrical) potential, μ_X^{SC} is the term representing the ion screening the charges around it, μ_X^{HS} is the excluded volume term, μ_X^{dehydr} is the ion's Gibbs free energy of hydration (Table 2), ϵ_{filter} is the filter dielectric constant, and ϵ_{bath} is the bath dielectric constant.

The excess chemical potential contains four terms in this model. An excluded volume portion (μ_X^{HS}) represents the chemical potential created by volume exclusion (i.e., two hard sphere ions cannot overlap). The electrostatic portion contains two parts, a mean electrostatic potential (V_D) and a screening component (μ_X^{SC}). The former is the long-time, many-particle average of the electrostatic potential, while the latter describes the energetic of ions rearranging to screen each other, with small ions lowering the free energy of the system because they screen better than larger ions that cannot approach as closely (Gillespie 2008). The dehydration term is represented as a Born scaling of the experimental Gibbs free energy of hydration with a dielectric constant, as was done previously by Nonner et al. (Nonner et al. 2001). For the bath, we have the concentrations of all ions within the system and we set the mean electrostatic potential to 0. This allows us to define the chemical potential for the bath μ_X^{bath} from the concentrations of the permeating ions. For the filter, however, the only concentration we know is that of the oxygens and the Donnan potential for the filter V_D is also a variable. To fill this gap, we assume charge neutrality in the filter because it is a bulk fluid. We can then numerically solve for the unknowns using Mathematica (version 7, Wolfram Research, Champaign, IL) to determine ionic concentrations in the filter and, thus, selectivity.

RESULTS

We considered selectivity of channels with filter ϵ_{filter} varying between 3 and 80 and oxygen concentration varying between 1 and 25 M with Li^+ , Na^+ , K^+ , Rb^+ , and Cs^+ present in the bath at 50 mM. 250 mM Cl^- was added in to the bath to balance out the charge from the cations. For each channel, we determined the selectivity sequence of the five cations by computing the concentration of each ion species in the filter. The sequences observed, listed in Table 1,

1
2
3
4 occurred in distinct regions as shown in Figure 1. Eight of the 11 Eisenman sequences were
5 observed and ten non-Eisenman sequences were observed (lowercase Roman numerals on Figure
6 1). Selectivity trended towards large ions at low dielectrics and low oxygen concentrations.
7

8 At high filter dielectric constants ($> \sim 75$), the oxygen concentration had no effect on
9 selectivity. However, at lower dielectrics increasing the oxygen concentration caused a trend
10 towards small ion selectivity (while keeping ϵ_{filter} fixed). This trend generally followed the
11 Eisenman sequences from I to XI with a few non-Eisenman sequences in a discrete band in the
12 middle of our data range. The higher oxygen concentration increased the weight of the hard
13 sphere and electrostatic terms in the chemical potential (Eq. (1)). The hard sphere portion
14 increased as oxygen concentration rose until volume exclusion became the dominant factor in
15 determining selectivity (Fig. 2). This figure shows, as a function of oxygen concentration, the
16 binding selectivity between K^+ and Na^+ which is defined by (Gillespie 2008)
17
18

$$\begin{aligned}
 \ln \left(\frac{[\text{K}^+]_{\text{filter}}}{[\text{Na}^+]_{\text{filter}}} \right) &= \overbrace{\ln \left(\frac{[\text{K}^+]_{\text{bath}}}{[\text{Na}^+]_{\text{bath}}} \right)}^{\text{number advantage}} + \overbrace{\frac{1}{kT} (\Delta\mu_{\text{K}}^{\text{SC}} - \Delta\mu_{\text{Na}}^{\text{SC}})}^{\text{screening advantage}} \\
 &+ \overbrace{\frac{1}{kT} (\Delta\mu_{\text{K}}^{\text{EV}} - \Delta\mu_{\text{Na}}^{\text{EV}})}^{\text{excluded-volume advantage}} \\
 &+ \overbrace{(\mu_{\text{K}}^{\text{dehydr}} - \mu_{\text{Na}}^{\text{dehydr}}) \frac{\epsilon_{\text{filter}} - \epsilon_{\text{bath}}}{\epsilon_{\text{filter}} (\epsilon_{\text{bath}} - 1)}}^{\text{dehydration advantage}}
 \end{aligned} \tag{2}$$

19
20
21
22
23
24
25
26
27
28
29
30
31
32 where the Δ indicates the difference between the filter and bath values of that component of the
33 chemical potential of ion X. A positive term in Eq. (2) favors K^+ binding in the filter while a
34 negative one favors Na^+ .
35

36 The figure shows each component of the binding selectivity of Eq. (2). The dehydration
37 term remains relatively constant and in favor of K^+ since the filter dielectric constant does not
38 change (from 50) during these calculations. As oxygen concentration increases, the hard sphere
39 term becomes larger and eventually increases to over four times the dehydration energy. Since
40 the entropic effect is so large, it is the main determinant of the selectivity of the system in this
41 region of the parameter space.
42

43 Changes to the dielectric constant of the filter produce a similar trend with large
44 dielectrics resulting in small ion selectivity (Fig. 3). Much like in the Fig. 2, this figure presents
45 difference in chemical potential and its components of Eq. (2), this time as a function of
46 dielectric constant in the filter. When the filter dielectric approaches that of the bath (78.4), the
47 dehydration penalties and the electrostatic interaction both approach 0. This means that the
48 excluded volume term becomes the largest determinant of electrochemical potential and thus
49 selectivity in the high ϵ_{filter} regime.
50

51 For small filter dielectrics, the picture gets a bit murkier. The screening component of
52 the chemical potential and dehydration both become very large and are of opposite sign, yet the
53 difference between the two is still relatively small. Therefore, small changes to how each term is
54 computed have large effects on the selectivity sequence observed. In order to accurately predict
55 sequences in this region, our model would need more detailed knowledge about the environment
56 of the channel and more accurate theories of the ions and their dehydration. While probably
57 inaccurate in this region, our model should produce the correct trend in selectivity for $\epsilon_{\text{filter}} \geq 15$.
58
59
60
61
62
63
64
65

1
2
3
4 While the vast majority of the selectivity sequences produced by the model are Eisenman
5 sequences, we also calculated a band of other sequences (the collection of lowercase Roman
6 numerals in Fig. 1). This band represents approximately 8.7% of channels with sequences that
7 do not match any of the 11 standard Eisenman sequences (or even the extended 13 Eisenman
8 sequences). They are broken down in a histogram in Fig. 4. Ten non-Eisenman sequences were
9 observed, but only five represented more than 1% of the total sequences (Table 1). These 10
10 sequences were generally Rb^+ or Na^+ selective while one was Li^+ selective. Despite being non-
11 Eisenman sequences they appeared in a distinct band of oxygen concentrations and dielectrics
12 (Fig. 1) and generally only had one pair of ions out of order when compared to an Eisenman
13 sequence that existed near that band.
14
15
16

17 DISCUSSION

18
19 We have shown that as we change the oxygen concentration and the dielectric constant of
20 the filter within our model, we observe many of the 11 Eisenman sequences in order. As oxygen
21 concentration increases, the sequences trend from I to XI (Table 1). As the dielectric constant
22 increases the sequences trend from XI to I.
23

24 Our model provides two definitions for field strength that correspond to these parameters.
25 A channel with a high oxygen concentration produces a “high field strength” sequence because it
26 increases the number of charges within the filter. Because of the steric effects caused by the
27 oxygens, a high $[\text{O}^{1/2-}]$ channel becomes small ion selective and produces a “high field strength”
28 sequence.
29

30
31 A low ϵ_{filter} means that water is excluded, increasing charge-charge interactions, and
32 thereby increasing field strength. However, we find that a high ϵ_{filter} produces an Eisenman
33 “high field strength” sequence. When the dehydration penalty is negligible ($\epsilon_{\text{filter}} > \sim 70$), the
34 channel is selective for small ions at virtually all oxygen concentrations. This appears to
35 contradict Eisenman’s definition of electrostatic field strength because a “high field strength”
36 selectivity sequence should imply increased charge-charge interaction. Increased charge-charge
37 interactions actually occur at low ϵ_{filter} instead of at high ϵ_{filter} in our calculations, the opposite of
38 what would be classically expected.
39

40
41 In Eisenman’s work the binding site charges were fixed in place because the binding site
42 was a glass (Eisenman 1962). However, calcium channels have mobile binding site charges.
43 This allows for some waters to enter. The filter dielectric constant this produces couples “field
44 strength” and the dehydration penalty. The field strength can be decreased by having more
45 waters around the screening charges. This extra water decreases charge-charge interactions
46 while simultaneously decreasing the magnitude of dehydration penalties. In Eisenman’s
47 calculations, the number of waters admitted into the channel did not affect selectivity. This is
48 because without an entropic term, the magnitude of the dehydration penalties would have to
49 become much smaller than we calculate before they would affect selectivity.
50

51
52 In the Eisenman model of a glass electrode, a single particle moving to a single binding
53 site has no entropic effect; the screening charge does not have to fit between other screening ions
54 and compete for space. However, this model of a rigid glass electrodes may not be a good
55 representation of a calcium channel that has amino acid side chains crowding the permeation
56 pathway. In our model, the excluded volume term is relatively constant as a function of ϵ_{filter} in
57 our chemical potential calculations (Fig. 3). Therefore, at high dielectric constants the relative
58
59
60
61
62
63
64
65

1
2
3
4 differences between the dehydration penalties would not alter selectivity because the hard sphere
5 term is so much larger than the dehydration penalties. Once entropic effects are included and
6 charge-charge interaction is coupled with dehydration energy through a dielectric constant, we
7 observe large ion selectivity in certain “high field strength” sites (Fig. 3).

8
9 While “field strength” may not work as a determinant of selectivity, our calculations
10 generally support the monotonic viewpoint of Armstrong (Armstrong 1989) when $\epsilon_{\text{filter}} > 15$.
11 Only a single peak in an affinity (ion concentrations in the filter) as a function of ionic diameter
12 is observed for all of the channels with Eisenman sequences, which were 91% of the observed
13 sequences. However, among the non-Eisenman sequences we computed, only one of the ten,
14 namely $\text{Rb}^+ > \text{K}^+ > \text{Na}^+ > \text{Cs}^+ > \text{Li}^+$ (iv), followed Armstrong’s argument. The other nine non-
15 Eisenman sequences depart from Armstrong’s argument and occurred mostly at very low
16 ($\epsilon_{\text{filter}} < \sim 15$) filter dielectric constants (Fig. 1). In fact, at extremely low filter dielectric constant
17 ($\epsilon_{\text{filter}} < \sim 8$) we found multiple peaks when affinity is plotted versus ionic radius (data not shown).
18 However, below $\epsilon_{\text{filter}} = 15$ our model is probably quite inaccurate because of the very large
19 attractive Coulombic forces and the very large repulsive dehydration penalties (Fig. 3). The
20 balance of these two large forces will always be hard to calculate, and our simple model is no
21 exception.
22
23
24

25 This parameter space region of low filter dielectric constant is also interesting because
26 these parameters characterize potassium channels. Potassium channels can generally be
27 described as excluding almost all waters and as having a large dipole and oxygen density (Doyle
28 et al. 1998). This describes exactly the lower region of Fig. 1 in which most of these sequences
29 occur. Our data shows K^+ versus Na^+ selectivity only in essentially gaseous environments (very
30 low oxygen concentration and ϵ_{filter}), which is consistent with gas-phase experiments of ion
31 binding with water molecules (Dzidic and Kebarle 1970). This seems to contradict the idea that
32 potassium channels have large oxygen concentrations and low dielectric constants. However,
33 theoretical studies on potassium channels show that the key difference between our high
34 oxygen/low dielectric channels and a potassium channel is the lack of constraint on oxygen
35 movement in our model; in the potassium channel the oxygens cannot move to fully coordinate
36 the permeating ions. A potassium channel’s filter charges are not present in the permeation
37 pathway as in our model and they do not move very freely as we allow our oxygens to do
38 (Fowler et al. 2008). This constraint on the oxygens’ ability to fully coordinate the permeating
39 ions produces K^+ selectivity over Na^+ . This data supports the argument that constraints on the
40 oxygens’ freedom of movement produces K^+ selectivity (Bostick and Brooks III 2007; Thomas
41 et al. 2007; Varma and Rempe 2007; Varma et al. 2008).
42
43
44
45
46

47 CONCLUSION

48 Our reduced model of a calcium channel produce eight of the eleven Eisenman
49 sequences, showing that the basic results of Eisenman continue to have staying power. The non-
50 Eisenman sequences we found were only 8.4% of the sequences we calculated. However,
51 contrary to Eisenman’s classic mechanism for these selectivity sequences, we found that in a
52 model with entropic, electrostatic, and dehydration components, electrostatic field strength does
53 not relate directly and monotonically to selectivity sequences. Specifically, two different model
54 parameters could be used to define a high field strength binding site, but they produced exactly
55 opposite selectivity sequences (I and XI). Since a real channel is much more complex than our
56 model, we conclude that the field strength characterization probably do not hold in real channels
57 as well.
58
59
60
61
62
63
64
65

1
2
3
4 **ACKNOWLEDGMENTS**
5

6 DG and DK were supported by NIH grant R01-AR054098. BE was supported in part by
7 NIH grant GM076013. We thank Sameer Varma for very useful discussions about potassium
8 channels and how they relate to our work.
9

TABLES

Table 1: List of all selectivity sequences observed in Fig. 1 with its percentage of the total.

Eisenman Sequences			Non-Eisenman Sequences		
seq. #	sequence	% total	seq. #	sequence	% total
I	Cs ⁺ >Rb ⁺ >K ⁺ >Na ⁺ >Li ⁺	9.29	i	Rb ⁺ >Na ⁺ >K ⁺ >Li ⁺ >Cs ⁺	0.002
II	Rb ⁺ >Cs ⁺ >K ⁺ >Na ⁺ >Li ⁺	5.64	ii	Rb ⁺ >Na ⁺ >K ⁺ >Cs ⁺ >Li ⁺	1.16
III	Rb ⁺ >K ⁺ >Cs ⁺ >Na ⁺ >Li ⁺	3.02	iii	Rb ⁺ >Na ⁺ >Cs ⁺ >K ⁺ >Li ⁺	0.006
IV	K ⁺ >Rb ⁺ >Cs ⁺ >Na ⁺ >Li ⁺	0	iv	Rb ⁺ >K ⁺ >Na ⁺ >Cs ⁺ >Li ⁺	2.70
V	K ⁺ >Rb ⁺ >Na ⁺ >Cs ⁺ >Li ⁺	0	v	Rb ⁺ >Cs ⁺ >Na ⁺ >K ⁺ >Li ⁺	0.003
VI	K ⁺ >Na ⁺ >Rb ⁺ >Cs ⁺ >Li ⁺	0	vi	Na ⁺ >Rb ⁺ >Li ⁺ >K ⁺ >Cs ⁺	0.14
VII	Na ⁺ >K ⁺ >Rb ⁺ >Cs ⁺ >Li ⁺	0.71	vii	Na ⁺ >Rb ⁺ >K ⁺ >Li ⁺ >Cs ⁺	1.01
VIII	Na ⁺ >K ⁺ >Rb ⁺ >Li ⁺ >Cs ⁺	2.76	viii	Na ⁺ >Rb ⁺ >K ⁺ >Cs ⁺ >Li ⁺	1.73
IX	Na ⁺ >K ⁺ >Li ⁺ >Rb ⁺ >Cs ⁺	0.59	ix	Na ⁺ >Li ⁺ >Rb ⁺ >K ⁺ >Cs ⁺	0.63
X	Na ⁺ >Li ⁺ >K ⁺ >Rb ⁺ >Cs ⁺	8.17	x	Li ⁺ >Na ⁺ >Rb ⁺ >K ⁺ >Cs ⁺	1.04
XI	Li ⁺ >Na ⁺ >K ⁺ >Rb ⁺ >Cs ⁺	61.40			
total		91.6	total		8.4

Table 2: Properties of all ions present in the system. Ion diameters are crystal diameters from Shannon and Prewitt (Shannon and Prewitt 1969) and the experimental Gibbs free energy of hydration are from Fawcett (Fawcett 1999).

ion	diameter (Å)	μ_x^{dehydr} (kJ/mol)
Li ⁺	1.33	-529.4
Na ⁺	2.00	-423.7
K ⁺	2.76	-351.9
Rb ⁺	2.98	-329.3
Cs ⁺	3.40	-306.1
Cl ⁻	3.62	-304.0
O ^{1/2-}	2.80	—

REFERENCES

- Armstrong CM (1989) Reflections on selectivity. In: Tosteson DC (ed) Membrane Transport: People and Ideas. American Physiological Society, Bethesda, MD, pp 261-273
- Barthel JMG, Krienke H, Kunz W (1998) Physical Chemistry of Electrolyte Solutions: Modern Aspects. Springer, New York
- Blum L (1975) Mean spherical model for asymmetric electrolytes I: Method of solution. Mol Phys 30:1529-1535
- Blum L (1980) Solution of the Ornstein-Zernike equation for a mixture of hard ions and Yukawa closure. J Stat Phys 22:661-672
- Boda D, Busath DD, Henderson D, Sokołowski S (2000) Monte Carlo simulations of the mechanism of channel selectivity: The competition between volume exclusion and charge neutrality. J Phys Chem B 104:8903-8910
- Boda D, Henderson D, Busath DD (2001) Monte Carlo study of the effect of ion and channel size on the selectivity of a model calcium channel. J Phys Chem B 105:11574-11577
- Boda D, Henderson D, Busath DD (2002) Monte Carlo study of the selectivity of calcium channels: Improved geometry. Mol Phys 100:2361-2368
- Boda D, Nonner W, Henderson D, Eisenberg B, Gillespie D (2008) Volume exclusion in calcium selective channels. Biophys J 94:3486-3496
- Boda D, Valiskó M, Eisenberg B, Nonner W, Henderson D, Gillespie D (2006) The effect of protein dielectric coefficient on the ionic selectivity of a calcium channel. J Chem Phys 125:034901
- Boda D, Valiskó M, Eisenberg B, Nonner W, Henderson D, Gillespie D (2007) Combined effect of pore radius and protein dielectric coefficient on the selectivity of a calcium channel. Phys Rev Lett 98:168102
- Boda D, Valiskó M, Henderson D, Eisenberg B, Gillespie D, Nonner W (2009) Ionic selectivity in L-type calcium channels by electrostatics and hard-core repulsion. J Gen Physiol 133:497-509
- Bostick D, Brooks III CL (2007) Selectivity in K^+ channels is due to topological control of the permeant ion's coordinated state. Proc. Natl. Acad. Sci. U S A 104:9260-9265
- Doyle DA, Morais Cabral J, Pfuetzner RA, Kuo A, Gulbis JM, Cohen SL, Chait BT, MacKinnon R (1998) The structure of the potassium channel: molecular basis of K^+ conduction and selectivity. Science 280:69-77
- Dzidic I, Kebarle P (1970) Hydration of the alkali ions in the gas phase: Enthalpies and entropies of reactions $M+(H_2O)_{n-1} + H_2O = M+(H_2O)_n$ J Phys Chem 74:1466-1474

- 1
2
3
4 Eisenman G (1962) Cation selective glass electrodes and their mode of operation. *Biophys J* 2
5 (Suppl. 2):259-323
6
7
8 Eisenman G, Alvarez O (1991) Structure and function of channels and channelogs as studied by
9 computational chemistry. *J Membr Biol* 119:109-132
10
11 Eisenman G, Horn R (1983) Ionic selectivity revisited: The role of kinetic and equilibrium
12 processes in ion permeation through channels. *J Membr Biol* 76:197-225
13
14
15 Fawcett WR (1999) Thermodynamic Parameters for the Solvation of Monatomic Ions in Water. *J*
16 *Phys Chem B* 103:11181-11185
17
18 Fowler PW, Tai K, Sansom MSP (2008) The selectivity of K⁺ ion channels: Testing the
19 hypotheses. *Biophys J* 95:5062-5072
20
21
22 Gillespie D (2008) Energetics of divalent selectivity in a calcium channel: The ryanodine
23 receptor case study. *Biophys J* 94:1169-1184
24
25
26 Gillespie D, Boda D (2008) The anomalous mole fraction effect in calcium channels: A measure
27 of preferential selectivity. *Biophys J* 95:2658-2672
28
29
30 Gillespie D, Boda D, He Y, Apel P, Siwy ZS (2008) Synthetic nanopores as a test case for ion
31 channel theories: The anomalous mole fraction effect without single filing. *Biophys J*
32 95:609-619
33
34
35 Gillespie D, Fill M (2008) Intracellular calcium release channels mediate their own
36 countercurrent: The ryanodine receptor case study. *Biophys J* 95:3706-3714
37
38
39 Gillespie D, Giri J, Fill M (2009) Reinterpreting the anomalous mole fraction effect: The
40 ryanodine receptor case study. *Biophys J* 97:2212-2221
41
42
43 Gillespie D, Xu L, Wang Y, Meissner G (2005) (De)constructing the ryanodine receptor:
44 Modeling ion permeation and selectivity of the calcium release channel. *J Phys Chem B*
45 109:15598-15610
46
47
48 Hille B (2001) *Ion Channels of Excitable Membranes*, 3rd edn. Sinauer Associates Inc.,
49 Sunderland
50
51
52 Koch SE, Bodi I, Schwartz A, Varadi G (2000) Architecture of Ca²⁺ channel pore-lining
53 segments revealed by covalent modification of substituted cysteines. *J Biol Chem*
54 275:34493-34500
55
56
57 Krasne S, Eisenman G (1973) The molecular basis of ion selectivity. In: Eisenman G (ed)
58 *Membranes: A Series of Advances: Lipid Bilayers and Antibiotics*, vol 2. Marcel Dekker,
59 New York
60
61
62
63
64
65

- 1
2
3
4 Malasics A, Gillespie D, Nonner W, Henderson D, Eisenberg B, Boda D (2009) Protein structure
5 and ionic selectivity in calcium channels: Selectivity filter size, not shape, matters.
6 Biochim Biophys Acta Biomembr 1788:2471-2480
7
8
9 Miedema H, Meter-Arkema A, Wierenga J, Tang J, Eisenberg B, Nonner W, Hektor H, Gillespie
10 D, Meijberg W (2004) Permeation properties of an engineered bacterial OmpF porin
11 containing the EEEE-Locus of Ca²⁺ channels. Biophys J 87:3137-3147
12
13
14 Miedema H, Vrouenraets M, Wierenga J, Gillespie D, Eisenberg B, Meijberg W, Nonner W
15 (2006) Ca²⁺ selectivity of a chemically modified OmpF with reduced pore volume.
16 Biophys J 91:4392-4400
17
18
19 Nonner W, Catacuzzeno L, Eisenberg B (2000) Binding and selectivity in L-type calcium
20 channels: A mean spherical approximation. Biophys J 79:1976-1992
21
22
23 Nonner W, Eisenberg B (1998) Ion permeation and glutamate residues linked by Poisson-Nernst-
24 Planck theory in L-type calcium channels. Biophys J 75:1287-1305
25
26
27 Nonner W, Gillespie D, Henderson D, Eisenberg B (2001) Ion accumulation in a biological
28 calcium channel: effects of solvent and confining pressure. J Phys Chem B 105:6427-
29 6436
30
31
32 Rodriguez-Contreras A, Nonner W, Yamoah EN (2002) Ca²⁺ transport properties and
33 determinants of anomalous mole fraction effects of single voltage-gated Ca²⁺ channels in
34 hair cells from bullfrog saccule. J Physiol 538:729-745
35
36
37 Shannon RD, Prewitt CT (1969) Effective ionic radii in oxides and fluorides. Acta Crystallogr
38 B25:925-946
39
40
41 Thomas M, Jayatilaka D, Corry B (2007) The predominant role of coordination number in
42 potassium channel selectivity. Biophys J 93:2635-2643
43
44
45 Varma S, Rempe S (2007) Tuning ion coordination architectures to enable selective partitioning.
46 Biophys J 93:1093-1099
47
48
49 Varma S, Sabo D, Rempe SB (2008) K⁺/Na⁺ selectivity in K channels and Valinomycin: Over-
50 coordination versus cavity-size constraints. J Mol Biol 376:13-22
51
52
53
54
55
56
57
58
59
60
61
62
63
64
65

FIGURE LEGENDS

1. Monovalent cation selectivity sequences for all channels with $[O^{1/2-}] = 1 \text{ M}$ to 25 M and $\epsilon_{\text{filter}} = 3$ to 80 . The five cations were each present at 50 mM in the bath along with 250 mM Cl^- . Roman numerals correspond to the selectivity sequences listed in Table 1. Capital numerals denote Eisenman sequences and lowercase non-Eisenman sequences.
2. Differences in the components of the electrochemical potential (Eq. (2)) between K^+ and Na^+ as a function of $[O^{1/2-}]$. The thin solid line corresponds to the screening advantage, the dotted line to the hard sphere advantage, the dashed line to the dehydration advantage, and the thick, solid line to the total of the other four lines, the overall binding selectivity. Positive values indicate the term favors K^+ over Na^+ accumulating in the filter while negative values indicate the opposite selectivity. The mean electrostatic and ideal gas components are the same for both ions and are not included. In this figure, $\epsilon_{\text{filter}} = 50$.
3. Differences in the components of the electrochemical potential (Eq. (2)) between K^+ and Na^+ as a function of ϵ_{filter} . The thin solid line corresponds to the screening advantage, the dotted line to the hard sphere advantage, the dashed line to the dehydration advantage, and the thick, solid line to the total of the other four lines, the overall binding selectivity. Positive values favor K^+ accumulating in the filter. The mean electrostatic and ideal gas components are the same for both ions and is not included. In this figure, $[O^{1/2-}] = 15 \text{ M}$.
4. Histogram of the data from Fig. 1. Each count is expressed as a percentage of the total number of sequences observed. Roman numerals correspond to the selectivity sequences in Table 1. Dark gray columns correspond to Eisenman sequences while light gray columns correspond to non-Eisenman sequences.

Figure 1

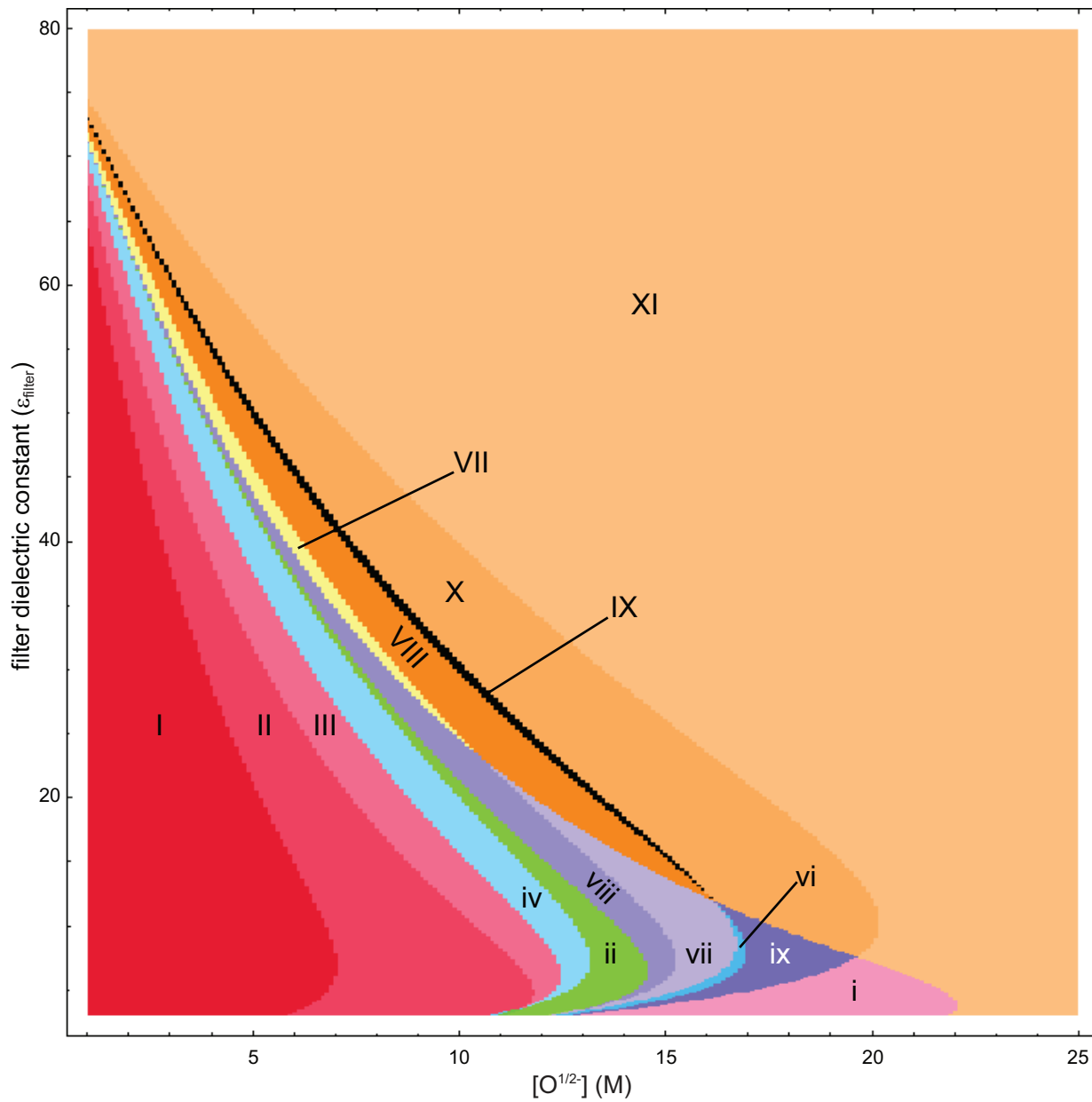


Figure 1

Figure 2

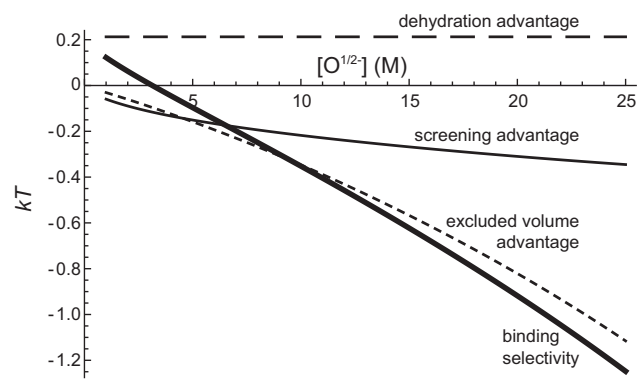


Figure 2

Figure 3

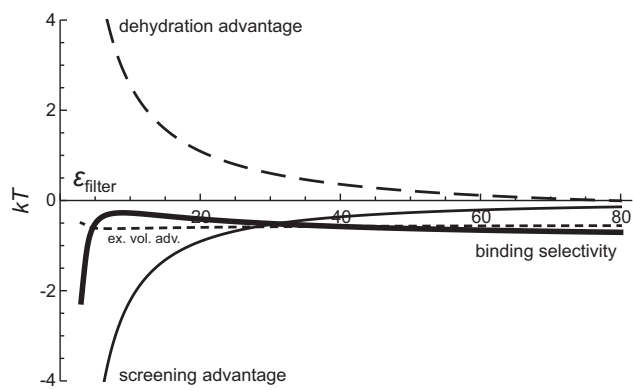


Figure 3

